

# Modeling aerodynamics for ultra-low Reynolds Number flight

Subham Kant Das and Sudipto Mukhopadhyay

Department of Mechanical Engineering, IIT Jodhpur, Jodhpur, 342037, India.

Corresponding Author: smukhopadhyay@iitj.ac.in

## Abstract

Micro Aerial Vehicles (MAVs) are increasingly being used for numerous applications such as surveillance, reconnaissance, agriculture, scientific missions and aerial photography. MAVs operate in ultra low Reynolds number regime characterized typically by Reynolds number less than 10,000. However, at (ultra) low Reynolds Number, the fluid particle doesn't have enough energy to overcome the adverse pressure gradient and thus separates. This leads to transition from laminar to turbulent regime and thus the fluid particle gains energy and reattaches to the surface, forming a separation bubble. The present study aims to evaluate the numerical modeling ability to capture this complex flow physics and quantify its influence on the aerodynamic performance parameters. The flow around a NACA0012 airfoil at an ultra-low Reynolds Number of 1000 is investigated using an open source Computational Fluid Dynamics (CFD) toolbox, OpenFOAM. Comparisons are made between the laminar and one-equation Spallart-Allmaras model on the basis of their ability to capture the flow behaviour at ultra-low Reynolds Number. A transition model that can address the effects of transition from laminar to turbulent regime has been implemented and efforts are made in order to generalize this model.

**Keywords:** NACA0012; OpenFOAM; ultra-low Reynolds Number; lift; drag; transition

## Introduction

MAVs compared to conventional aircrafts offer advantages of cost-effectiveness, higher payload capacity, and portability. However, there is an upper limit to the maximum altitude they can achieve as they operate on Reynolds number less than 10000, where a significant amount of lift is not generated. Lissaman[1] presented a comparison of the performance of airfoils at different Reynolds number. He concluded that airfoils fail to operate at a Reynolds number below 100 due to the dominant viscous effect and demonstrate a relatively weaker performance at a Reynolds number of the order  $10^5$ . Beyond this value, where most of the modern aircraft operate, there is a significant enhancement in the performance of the airfoil. At low Reynolds Number, the viscous effects are predominant, leading to flow separation and reattachment, which further increases the drag force, and lowers the lift. At higher Reynolds, Number viscous effects are less dominant, and hence, there is a significant improvement in the flow characteristics.

McMasters and Henderson[2] studied this transition of the performance of airfoils and determined the critical Reynolds number to be close to 70000 beyond which there is a change in the performance of airfoils. At lower Reynolds number, airfoils with rough surface showed better performance when compared to smooth ones. For rough airfoils, the performance increases linearly with an increase in the Reynolds Number. However, the effect of smoothness becomes significant after a Reynolds Number of  $10^5$ . At higher Reynolds number (of the order of  $10^6$ ), the drag coefficient remains constant with an increase in lift. But at the mid-range, the flow behavior is quite complicated due to the introduction of flow separation and reattachment. Hence larger values of drag are obtained for moderate angles of attack.

The wings of the MAVs are derived from airfoils and the aerodynamic forces are characterized by the lift and drag coefficients of the airfoils. The accurate and efficient determination of the aerodynamic forces on wings due to relative fluid motion are essential for the design and development of MAVs. It is relatively easier to predict the flow behaviour at the higher Reynolds numbers corresponding to fully turbulent flow since there is delayed or no separation at all. However, at lower Reynolds Number, the fluid particle doesn't have enough energy to overcome the adverse pressure gradient and thus, separates. This leads to transition from laminar to turbulent regime and thus the particle gains energy and reattaches to the surface, forming a separation bubble. These effects becomes more predominant at higher angles of attack where conventional model fails to predict the flow physics. The flow around an airfoil at ultra-low Reynolds number is an interesting field to study as it has many practical applications. As discussed above, the performance of an airfoil is not better in this operational range.

The study aims not only to evaluate the numerical procedure on the basis of its ability to capture flow physics but also to quantify the influence of the parameters contained within the modelling procedure. The effect of boundary proximity and mesh resolution has been studied in detail. Comparisons are made in reference to the experimental conducted by Liu. et. al[3]. The results obtained can be used to identify the most novel parameter that would provide accurate results with great computational efficiency. Comparisons are made between the laminar and one-equation Spalart Allmaras model on the basis of their ability to capture the flow behaviour at ultra-low Reynolds Number. A transition model that can address the effects of transition from

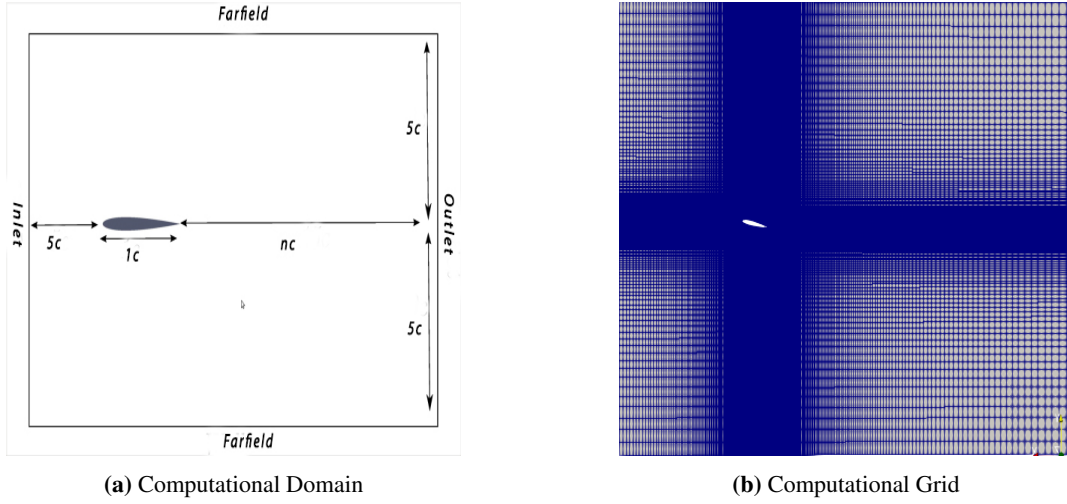


**Figure 1:** Computational domain and grid used for the present study

laminar to turbulent regime has been implemented in open source code, OpenFOAM and efforts are made in order to generalize this model.

## Computational Methodology

An open source Computational Fluid Dynamics (CFD) toolbox, OpenFOAM is used for simulations in the present paper. The governing equations for the flow problem are the continuity and the momentum equations. For turbulent flows, these equation needs to include sub models for turbulent closure. In CFD, RANS is the most widely used turbulence modeling approach. In this approach, velocity and pressure are split into mean and fluctuating components. There are several models available which take into account the effect of turbulence, the number of equation ranges from one to many depending on the model. In the present study, since the Reynolds number is 1000 laminar flow is a natural choice. Further Spalart-Allmaras (SA) [4] model, a one-equation model that solves a modelled transport equation for the kinematic eddy turbulent viscosity is also considered. The SA model was designed specifically for aerospace applications involving adverse pressure gradients. It solves a transport equation for a viscosity-like variable  $\tilde{\nu}$ . This may be referred to as the SA variable. The turbulent viscosity can be obtained from this variable by using the following relation:

$$\nu_t = \tilde{\nu} f_{v1}$$

where,  $f_{v1}$  is the viscous damping function.

The governing equations for the RANS approach based on the one-equation Spalart-Allmaras model are given by:

$$\nabla \cdot U = 0 \quad (1)$$

$$\frac{\partial U_i}{\partial t} + \nabla \cdot (U_i U) = -\frac{1}{\rho} \frac{\partial P}{\partial x_i} + \nabla \cdot (\nu \nabla U_i) - \frac{\partial \tau_{ij}}{\partial x_j} \quad (2)$$

$$\frac{\partial \tilde{\nu}}{\partial t} + u_j \frac{\partial \tilde{\nu}}{\partial x_j} = C_{b1} [1 - f_{t2}] \tilde{S} \tilde{\nu} + \frac{1}{\sigma} \{ \nabla \cdot [(\nu + \tilde{\nu}) \nabla \tilde{\nu}] + C_{b2} |\nabla \tilde{\nu}|^2 \} - \left[ C_{w1} f_w - \frac{C_{b1}}{\kappa^2} f_{t2} \right] \left( \frac{\tilde{\nu}}{d} \right)^2 + f_{t1} \Delta U^2 \quad (3)$$

where,

$$\tilde{S} \equiv S + \frac{\tilde{\nu}}{\kappa^2 d^2} f_{v2}, \quad f_{v2} = 1 - \frac{\chi}{1 + \chi f_{v1}}$$

$$f_w = g \left[ \frac{1 + C_{w3}^6}{g^6 + C_{w3}^6} \right]^{1/6}, \quad g = r + C_{w2} (r^6 - r), \quad r \equiv \frac{\tilde{\nu}}{\tilde{S} \kappa^2 d^2}$$

$$f_{t1} = C_{t1} g_t \exp \left( -C_{t2} \frac{\omega_t^2}{\Delta U^2} [d^2 + g_t^2 d_t^2] \right), \quad f_{t2} = C_{t3} \exp(-C_{t4} \chi^2), \quad S = \sqrt{2 \Omega_{ij} \Omega_{ij}}, \quad \Omega_{ij} = \frac{1}{2} (\partial u_i / \partial x_j - \partial u_j / \partial x_i)$$

The computational domain used for the purpose of the present study is shown in Figure 1(a). For eliminating domain extent effects the length of the domain beyond the trailing edge of the airfoil was considered as a variable. The length of the domain

behind the trailing of the airfoil edge were chosen as  $10c$  and  $15c$ , where  $c$  is the chord length of the airfoil in metres. The grid was generated using the blockMeshDict utility available in OpenFOAM. The mesh generation using blockMesh is swift as well as flexible. Figure 1(b) shows the computational grid generated from the blockMeshDict utility. Flow over NACA0012 airfoil at different angles of attack (AoA) is simulated for Reynolds number of 1000. The open-source software OpenFOAM is used for the simulations on a 2-D computational domain. The continuity and momentum equation is solved at the cell center of the control volume, and the required variables are computed at each cell center.

## Results and discussions

### Computational domain extent and mesh convergence

It is necessary to have sufficient length of the domain behind the trailing edge of the airfoil in order to capture the wake. It also helps in proper convergence of the solution. But having a larger domain size may increase the computation time significantly. An objective of the study was to come up with an optimum domain size that would be able to predict the lift and drag characteristics of the airfoil and at the same time provide better computational efficiency. For the purpose of the present study, two different computational domains were taken into consideration. The length of the domain behind the trailing of the airfoil edge was taken to be  $10c$  and  $15c$  respectively, where  $c$  is the chord length of the airfoil in metres. The number of cells meant to capture the flow near the wall was kept constant for all the cases. However, increase in the length of domain beyond the trailing edge of the airfoil increased the mesh count as well which, in turn, led to an increase in computational time. The results obtained using both the laminar and Spalart Allmaras model are compared with the experiments conducted by Liu et al. [3] at a Reynolds Number of 1000 and Angle of Attack of 5 degrees for which the results are shown in Table 1. The velocity contour obtained for both the model is shown in Figure 2. It was observed that there was negligible effect of increasing the domain size on the numerical results and hence our model can be considered to be domain independent. Hence, for further investigations streamwise domain extent was taken as  $10c$ .

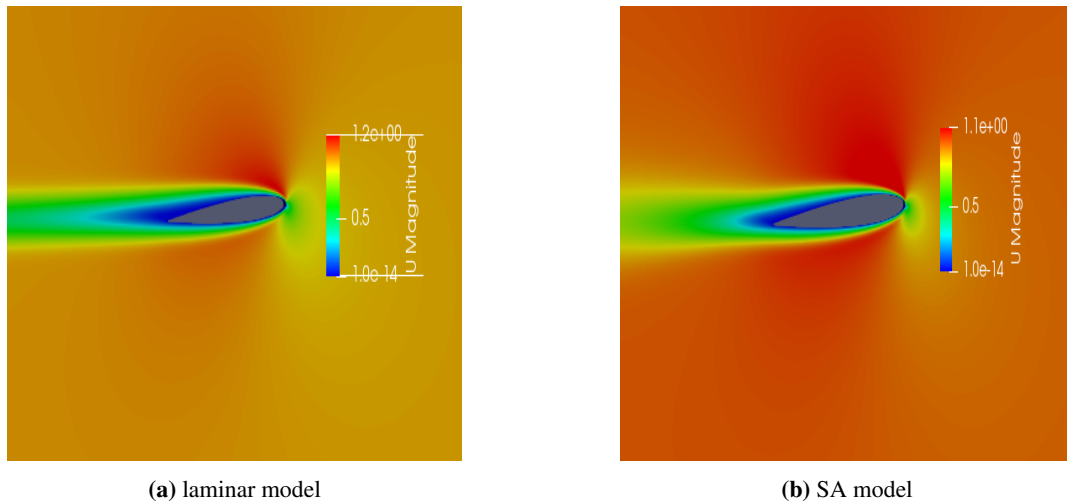


**Figure 2:** velocity contour obtained from laminar and SA model at an AoA of 5 degree

Size of Domain	Angle of Attack	$C_L Num$	$C_L Expt$	Percent Error	$C_D Num$	$C_D Expt$	Percent Error
<b>laminar</b>							
10c	5°	0.2342	0.24	2.41	0.1279	0.128	0.07
15c	5°	0.2342	0.24	2.41	0.1279	0.128	0.07
<b>Spalart Allmaras</b>							
10c	5°	0.244	0.24	2.08	0.1286	0.128	2.427
15c	5°	0.244	0.24	2.08	0.1286	0.128	2.427

**Table 1:** Comparison of numerical results with the experimental data at different domain extension (Re=1000)

To ensure that the solutions are independent of the mesh resolution, grid independence test was conducted using the laminar model (since it performed better than the Spalart Allmaras model at an AoA of 5 degrees) for a domain extent of  $10c$  beyond the

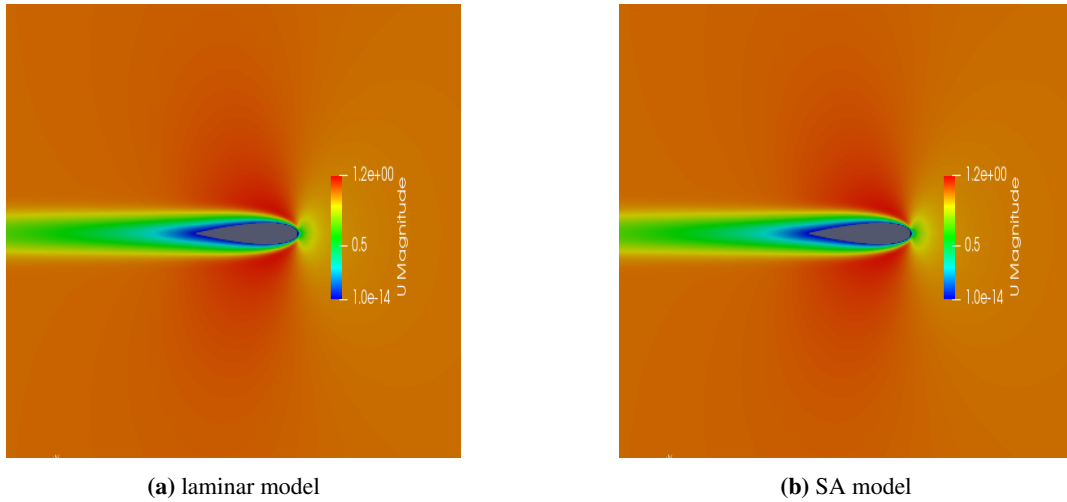


**Figure 3:** velocity contour obtained from laminar and SA model at an AoA of 0 degree

trailing edge of the airfoil. Three different grids were taken into consideration consisting of 27150, 108600, and 434400 cells respectively. The data used for validation was that of Liu et. al.[3] at a Reynolds number of 1000 and an angle of attack of 5 degrees.

As evident from Table 2, the coarser grid over-predicted the lift coefficient and under-predicted the drag coefficient while the results obtained using fine and very fine mesh were the same. The simulation time taken for the very fine mesh was very large due to which the finer mesh having 108600 cells was selected for computational purpose. and as evident from table 2, that the solutions were independent of the grid resolution.

	Number of Cells	Angle of Attack	$C_L Num$	$C_L Expt$	Percent Error	$C_D Num$	$C_D Expt$	Percent Error
1	27150	5°	0.283	0.24	17.9	0.103	0.128	19.5
2	108600	5°	0.2342	0.24	2.41	0.1279	0.128	0.07
3	434400	5°	0.2342	0.24	2.41	0.1279	0.128	0.07

**Table 2:** Comparison of numerical results with the experimental data at different refinement levels

### Performance of Laminar and SA Model

Both laminar and the one equation SA model was used for performing the simulation at a Reynolds Number of 1000 and different Angles of Attack and comparisons were made between the two on the basis of their ability to capture the flow physics in reference to the experiments conducted by Liu. et. Al. The lift and drag coefficient data and the percentage error between the numerical and experimental results have been shown in Table 3 and the velocity contour has been shown in Figure 2, 3, and 4.

	Angle of Attack	$C_L Num$	$C_L Expt$	Percent Error	$C_D Num$	$C_D Expt$	Percent Error
<b>laminar</b>							
1	0°	0	0	–	0.1199	0.12	0.08
2	5°	0.2342	0.24	2.41	0.1279	0.128	0.07
3	10°	0.339	0.421	19.4	0.15176	0.17	10.72
<b>Spalarat Allmaras</b>							
1	0°	0	0	–	0.1182	0.12	1.5
2	5°	0.244	0.24	1.6	0.1286	0.128	0.4
3	10°	0.5457	0.421	29.6	0.2238	0.17	31.6

**Table 3:** Comparison between the laminar and SA model for a Reynolds Number of 1000 and different AoA

It was observed that the ability of the laminar model to predict the lift and drag coefficient decreased with an increase in AoA and at an AoA of 10°, it completely failed to predict the flow behaviour. The ability of SA model to predict the flow physics, started to increase till an AoA of 5°, however it too failed to predict the lift and the drag coefficient at an AoA of 10°. This was attributed to the fact that at lower Reynolds number, the flow is laminar and has less energy due to which it fails to maintain

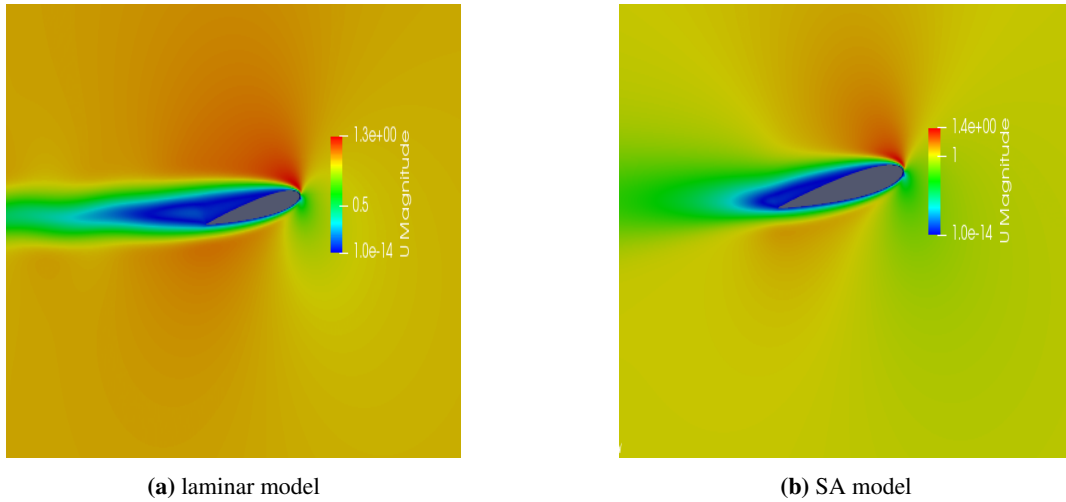


**Figure 4:** velocity contour obtained from laminar and SA model at an AoA of 10 degree

contact with the surface of the airfoil, leading to separation. This separation ultimately leads to transition to turbulent regime where the flow gains energy and reattaches to the surface of the airfoil thus forming a laminar separation bubble. Thus arises the need of a model that can address the transition from laminar to turbulent regime.

**Performance of Transition Model**

An important observation made from Table 3 was that the laminar model under-predicted the lift and the drag coefficient whereas the SA model over-predicted them. Since, the conventional models failed to predict the flow behaviour at an AoA of 10 degrees, the exact point of separation could not be identified. Hence the the separation point was arbitrary chosen and based on the results obtained, the separation point could be shifted either towards the laminar or towards the turbulent regime.

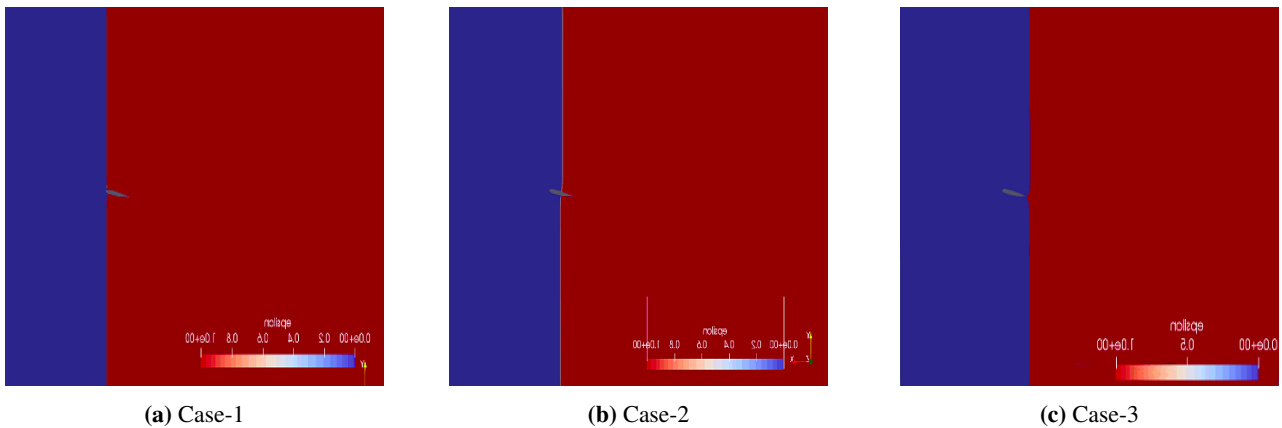


**Figure 5:** Laminar and turbulent zones for case-1, case-2, and case-3

As shown in figure 5, three arbitrary location were taken into consideration, one near the leading edge, one at the center and one near the trailing edge of the airfoil. We might refer to them as Case-1,2, and 3 respectively. In order to take the effect of separation into consideration, the transition model aimed to divide the computational domain into two zones, viz., laminar and turbulent as shown in Figure 6. A closer view of the laminar and turbulent zones has been shown in Figure 7. A new variable  $\alpha$  was defined which was assigned a value of zero in the laminar zone and one in the turbulent zone. This  $\alpha$  was then multiplied with the turbulent kinematic viscosity ( $\nu_t$ ), thus forcing it to be zero in the laminar region.

RAS Model	$C_L Num$	$C_L Expt$	Percent Error	$C_D Num$	$C_D Expt$	Percent Error
<b>AoA=10°</b>						
laminar	0.339	0.421	19.4	0.15176	0.17	10.72
SA	0.5457	0.421	29.6	0.2238	0.17	31.6
case-1	0.52	0.421	23.5	0.203	0.17	19.4
case-2	0.49	0.421	16.3	0.192	0.17	12.9
case-3(modified model)	0.4439	0.421	5.4	0.1727	0.17	1.58

**Table 4:** Comparison of numerical results with the experimental data for different models studied

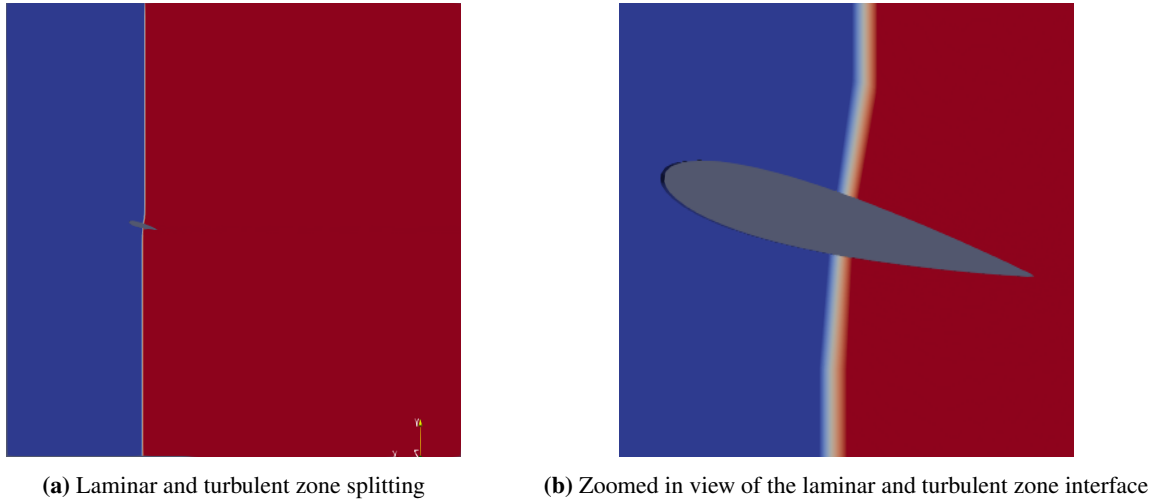


**Figure 6:** Splitting of the domain into laminar ( $\nu_t = 0$ ) and turbulent regime ( $\nu_t \neq 0$ )

It can be observed from Table 4 that the modified model with the point of separation located near the trailing edge of the airfoil(case-3) was able to predict the lift and the drag coefficient with a reasonable amount of accuracy. It can be observed from Figure 7 how the modified model forces the turbulent kinematic viscosity to zero in the laminar region.

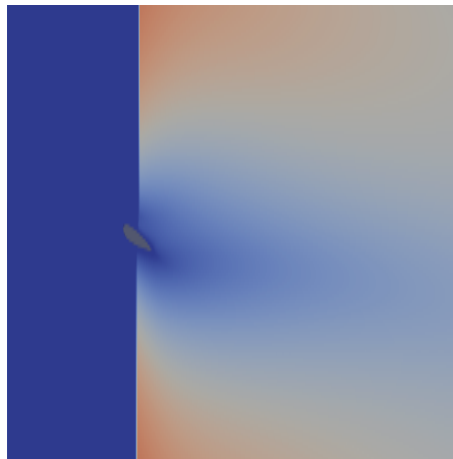


**Figure 7:** The modified model forcing  $\nu_t$  to zero in the laminar zone

In order to investigate this further, the streamlines for the laminar(Fig. 8a), SA(Fig. 8b) and the modified model with the separation point located near the trailing edge (Fig. 8c) was plotted. It can be easily observed from Fig. 8 that the laminar model predicted the onset of separation quite early with a re-circulation bubble near the center of the airfoil, which led to a lesser lift coefficient. The SA turbulent model however delayed the onset of separation and there was no separation bubble observed, which led to an overestimation of lift coefficient. The modified model, however displayed a small re-circulation zone near the trailing edge which was in agreement with the experiments.

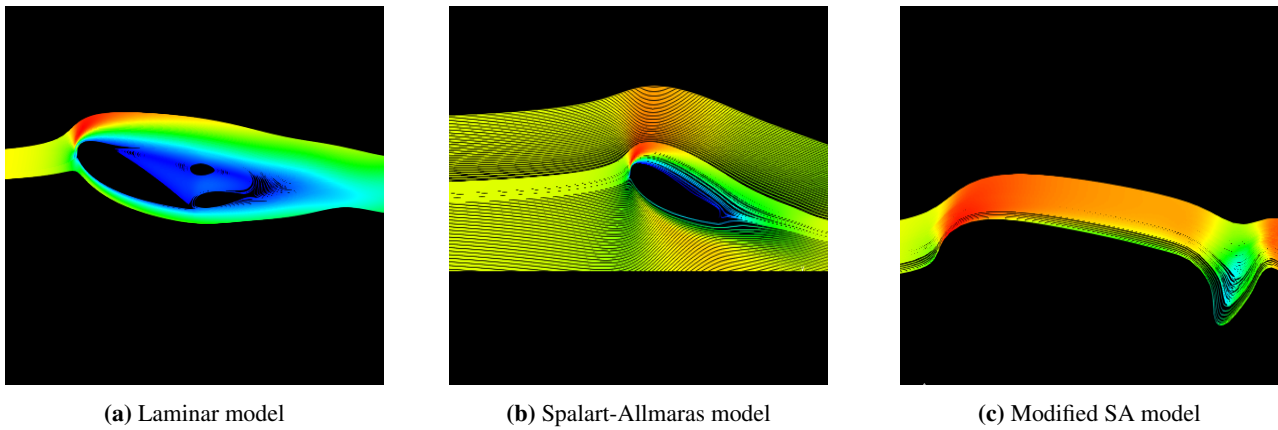


**Figure 8:** The streamlines obtained for various models showing the point of separation and the separation bubble

## Conclusion

Aerodynamic forces given by lift and drag coefficient for ultra low Reynolds number flow over a symmetric airfoil were investigated using OpenFOAM. It was found the results were not satisfactory by assuming a fully laminar or fully turbulent flow. A modified turbulence model was implemented which divided the computational domain into laminar and turbulent model zones. This resulted a better agrrement with experimental results. However, the point of demarcation was chosen on trail basis. Further research is required in order to generalize this model to estimate the domain bifurcation and predict the onset of separation with higher confidence.

## References

- [1] PBS Lissaman, Low Reynolds Number Airfoils.
- [2] McMasters, J.H. Henderson, Low speed single element airfoil synthesis, Technical Soaring, Vol.6, No. 8, 1980
- [3] Y. Liu, K. Li, J. Zhang, H. Wang, L. Liu, Numerical bifurcation analysis of static stall of airfoil and dynamic stall under unsteady perturbation
- [4] Spalart, P. R. and Rumsey, C. L., "Effective Inflow Conditions for Turbulence Models in Aerodynamic Calculations," AIAA Journal, Vol. 45, No. 10, 2007, pp. 2544-2553